

AGILE: An innovative instrument concept to identify and characterize solar energetic particles

Shrikanth G Kanekal¹, Christophe Royon², Doumerg W. d'Assignies², Florian Gautier², Ashley D Greeley³, Tommaso Isidori², Nicola Minafra², Alexander Novikov², Eric Oberla⁴, Quintin Schiller⁵, and Robert Young⁶

¹National Aeronautics and Space Administration (NASA)

²Department of Physics and Astronomy, University of Kansas

³NASA Goddard Space Flight Center

⁴Kavli Institute for Cosmological Physics

⁵NASA, Goddard Space Flight Center

⁶Instrumentation Design Laboratory, University of Kansas

November 24, 2022

Abstract

We describe a novel particle telescope, the Advanced enerGetic Ion eLectron tElescope (AGILE), which utilizes full pulse shape discrimination to identify solar energetic particles (SEP), and characterizes their spectra from about 2 to 200 MeV/nuc for most species from H to Fe. AGILE is a compact, low mass, and low-power particle telescope suitable for CubeSat platforms that enable multi-point measurements in interplanetary space. AGILE will employ high heritage solid state detectors, a state-of-art high-speed sampling ASIC, as well as novel algorithms to characterize SEP to advance the understanding of charged particle energization, loss, and transport throughout the heliosphere. AGILE will resolve ion isotopes (e.g. ^3He vs. ^4He) with high robustness and reliability. Currently, a prototype of the instrument is being built and will be part of science payload on the GenSat-1 CubeSat. GenSat-1 is expected to be launched early 2022 into a high inclination low earth orbit, with AGILE collecting data over the polar regions, i.e., the open field line regions accessed by SEP.

1 **AGILE: An innovative instrument concept to identify**
2 **and characterize solar energetic particles**

3 **S.G. Kanekal¹, C. Royon², W. d'Assignies D.^{2,5}, F. Gautier², A. Greeley¹, T.**
4 **Isidori², N. Minafra², A. Novikov², E. Oberla⁴, Q. Schiller⁴, R. Young³**

5 ¹Heliophysics Division, NASA Goddard Space Flight Center, Greenbelt, MD

6 ²Department of Physics and Astronomy, University of Kansas, Lawrence, KS

7 ³Instrumentation Design Laboratory, University of Kansas, Lawrence, KS

8 ⁴Space Science Institute, Boulder, CO

9 ⁴Dept. of Physics, Enrico Fermi Inst., Kavli Inst. for Cosmological Physics, University of Chicago,

10 Chicago, IL

11 ⁵Physics institute of the Ecole Normale Supérieure PSL, Paris, France

12 **Key Points:**

- 13
- 14 • Solar Energetic Particles
 - 15 • Particle identification (PID) of ion species from H to Fe
 - Full pulse shape discrimination (PSD) to identify ions

Abstract

We describe a novel particle telescope, the Advanced enerGetic Ion eLEctron tElescope (AGILE), which utilizes full pulse shape discrimination to identify solar energetic particles (SEP), and characterizes their spectra from about 2 to 200 MeV/nuc for most species from H to Fe. AGILE is a compact, low mass, and low-power particle telescope suitable for CubeSat platforms that enable multi-point measurements in interplanetary space. AGILE will employ high heritage solid state detectors, a state-of-art high-speed sampling ASIC, as well as novel algorithms to characterize SEP to advance the understanding of charged particle energization, loss, and transport throughout the heliosphere. AGILE will resolve ion isotopes (e.g. ^3He vs. ^4He) with high robustness and reliability. Currently, a prototype of the instrument is being built and will be part of science payload on the GenSat-1 CubeSat. GenSat-1 is expected to be launched early 2022 into a high inclination low earth orbit, with AGILE collecting data over the polar regions, i.e., the open field line regions accessed by SEP.

Plain Language Summary

When a charged particle passes through a solid state detector, it ionizes and knocks off electrons and “holes” (lack of electrons) from the detector material, such as silicon. These charges migrate to the edges of the detector under the influence of an electric field, arising from an applied bias voltage and result in small electrical signal. These small signals are amplified and their amplitude (pulse height) are measured, providing information regarding particle characteristics. Stacks of such solid state detectors called particle telescopes have been used in space physics for a long time to measure radiation belt electrons and protons, solar energetic ions, and galactic cosmic rays. However, using only the amplitude neglects the information that resides in the shape of the pulse, which can be used to identify ion species. Such a technique is called pulse shape discrimination (PSD). AGILE will be the first instrument to employ this technique in space to measure particle energy and species by utilizing recent advancements in electronics such as ASICs (Application Specific Integrated Circuit). These modern low power ASICs can characterize pulse shapes due to their high sampling rates making them ideal for space applications.

1 Introduction

In order to understand the physical processes underlying charged particle energization, loss, and transport throughout the heliosphere, in-situ measurements of particle intensities, spectra, and pitch angle, as well as clear identification of particle species are needed (Klecker, 2009). Broad classes of particle energization in the heliosphere include shock acceleration, coherent electric field acceleration, and stochastic acceleration (Council, 2004). For example, interplanetary shocks (e.g., leading coronal mass ejections (CME) and corotating interaction regions (CIR)) as well as magnetic reconnection (solar flares) are responsible for accelerating charged particles from the sun (Desai & Giacalone, 2016). Within the terrestrial radiation belts, a plethora of wave-particle processes energize electrons to relativistic energies (Horne et al., 2005; Thorne, 2010; Fennell et al., 2014), while radial diffusion - often driven by ultra low frequency (ULF) waves - is also an important mechanism (Falthammar, 1965; Shprits et al., 2008; Schulz & Lanzerotti, 1974). In solar energetic particle (SEP) events, elemental abundances provide valuable information regarding SEP acceleration, coronal source region, and solar wind composition, e.g., via fractionation (Reames, 2017). Classification of SEP events into impulsive and gradual types - for example finding flare type material in large gradual SEP, $^3\text{He}/^4\text{He}$ and Fe/O, Fe/C ratios - are a paradigm shift that emphasizes the need for unambiguous species identification (Desai & Giacalone, 2016; Klecker, 2009).

65 Traditional instrumentation covering energetic SEP ions in the range of tens of MeV/n,
 66 e.g., the HET (High Energy Telescope) instrument on STEREO (Solar Terrestrial Re-
 67 lations Observatory) (von Roseninge et al., 2008) and SIS (Solar Isotope Spectrome-
 68 ter) instrument on ACE (Advanced Composition Explorer) (Stone et al., 1998b), are usu-
 69 ally solid-state detector particle telescopes relying on a dE/dx-E technique (Stone et al.,
 70 1977). The basic dE/dx-E method requires at least two detector elements (the first one
 71 is usually thin and the second thick) and uses only the pulse height information, viz.,
 72 dE, the energy deposited by the particle passing through the first detector element, and
 73 E, the energy deposited by this particle completely stopping in the second element (see
 74 for example, (Goulding & Harvey, 1975)). A refinement of this technique was employed
 75 by the ACE-SIS and STEREO-LET (Low Energy Telescope) and HET instruments. Full
 76 details of this technique is described in Stone et al. (1998a). While this newer technique
 77 improved for example, the isotope resolution, it still relied on measuring only the energy
 78 deposited by the incident ionizing charged particle.

79 However, it is well known that in a single fully depleted solid state detector (e.g.
 80 Si) the shape of the pulse that is generated by a particle completely stopping in a de-
 81 tector contains information that can be used to identify its species (Mutterer et al., 2000).
 82 This information has long been used in nuclear physics applications for accelerator ex-
 83 periments (Ammerlaan et al., 1963; Carboni et al., 2012). This method, called pulse shape
 84 discrimination (PSD), utilizes the full shape of the signal (not just the amplitude, as is
 85 typical in space-based instrumentation) arising from a particle passing through the de-
 86 tector elements and will be used by the AGILE instrument for the first time in space.
 87 The aforementioned nuclear physics applications used bulky detectors and associated elec-
 88 tronics which had high power consumption and therefore are not suitable for space based
 89 applications. Recent developments in low power high time resolution electronics has made
 90 it possible to design low power low mass instrumentation employing the PSD technique. The
 91 key development enabling AGILE has been low power high sampling rate ASICs (Ap-
 92 plication Specific Integrated Circuits). AGILE will leverage these recent developments
 93 to obtain particle ID and energy implementing the PSD technique. Critical components
 94 of AGILE, such as the sampling ASIC, have already been fully tested and utilized in high
 95 energy physics experiments. An AGILE instrument prototype is slated to fly on Gensat-
 96 1, a CubeSat to be launched into high inclination LEO, while a full version is planned
 97 for future missions.

98 As will be referred to and noted throughout this paper, the AGILE team has car-
 99 ried detailed simulations of the full detection chain (Gautier et al., 2021). These sim-
 100 ulations cover the complete detection process starting from particle interaction with de-
 101 tectors including generation of pulses within the detectors to the final electronic ampli-
 102 fier output. The simulation chain uses the Geant4 toolkit (Agotstinelli, 2003) to simu-
 103 late particle interaction with matter, Weightfield2 (Cenna et al., 2015) to simulate sig-
 104 nal characteristics within the detector material (e.g., Silicon), and LTspice (commerci-
 105 ally available software) for the front end electronics.

106 AGILE measurements of interplanetary ions will cover energy ranges critical to the
 107 understanding of SEPs and anomalous cosmic rays (ACRs) with high robustness and re-
 108 liability. These improved measurements of SEPs will further our understanding of the
 109 acceleration and transport of charged particles in the inner heliosphere, whereas improved
 110 measurements of ACRs explore processes in the remote heliosphere, namely, the termi-
 111 nation shock and the heliosheath. Within the magnetosphere, AGILE can, for the first
 112 time, unambiguously distinguish between electrons and protons and probe the question
 113 of relativistic electron injection into the inner zone, which remains currently an open and
 114 controversial topic.

115 This paper describes the science goals, design, implementation, calibration, and ex-
 116 pected data products of the prototype AGILE instrument. Following the introduction,
 117 Section 2 describes the science goals to be addressed by AGILE, with the general aspects

Table 1. Science traceability matrix for AGILE

Science Goals and Science Objectives	Measurement Requirements	Instrument Requirements	Projected performance	Mission Requirements
1. Energization, transport and modulation of IP charged particles 1.1 Study SEP and ESP energization at IP shocks 1.2 Study ACR transport and modulation	Spectra & time-intensity profiles of SEP ions H to Fe from ≈ 2 to 100 MeV/nuc with sufficient energy (<50%) and time resolution (<5 minutes)	Ions H to Fe >5 differential energy channels $\Delta E/E \sim 30\%$ Sufficiently large geometry factor	>8 differential energy channels $\Delta E/E \sim 30\%$ Geometry factor $\approx 0.61 \text{ cm}^2\text{-sr}$ Excellent particle species identification with state of the art digital signal processing (S/N >20)	Interplanetary space, e.g., L1 Lagrange point OR High-inclination LEO [‡] High-inclination LEO [‡]
2. Space weather aspects of IP energetic particles 2.1 Study proton and ion cutoffs during geomagnetically disturbed times 2.2 Characterize particle spectra during intense SEP events				
3. Study the dynamics of energetic electrons in the Earth's Radiation Belts 3.1 Characterize trapped and transient energetic ion populations in the outer zone 3.2 Determine presence and characterize relativistic electrons in the inner zone	Intensities and spectral measurements of ≈ 1 -10 MeV electrons with sufficient energy (<50%) and time resolution (<1 minutes)	Electrons >5 differential energy channels $\Delta E/E \sim 30\%$ optimized geometry factor to cover relativistic and ultra-relativistic electron intensities	>8 differential energy channels $\Delta E/E \sim 30\%$ Geometry factor $\approx 0.61 \text{ cm}^2\text{-sr}$ Excellent electron-ion separation (S/N >20)	High-inclination LEO [‡] OR Near-equatorial GTO [†]

[‡]LEO: Low earth Orbit, [†]GTO: Geosynchronous Transfer Orbit

118 of particle identification by the PSD technique delineated in Section 3. The details of
 119 AGILE's implementation are described in Section 4 including the solid state detectors
 120 and the front end electronics (FEE, Section 4.1). The sampler chip which is the heart
 121 of the PSD technique (Section 4.3) and the onboard processing (Section 4.4) are also de-
 122 scribed in Section 4. Section 5 describes the calibration and Section 6 details the data
 123 products of AGILE. The flight opportunity for AGILE is described briefly in Section 7
 124 followed by a summary in Section 8.

125 2 Science Objectives and Goals

126 The space-based application of the pulse shape discrimination method allows sci-
 127 entific advancement in three major topics regarding our understanding of charged par-
 128 ticle dynamics in the solar system from a low-Earth orbit (LEO). Specifically, 1) ener-
 129 getic particles originating from the Sun, 2) low energy cosmic rays including anomalous
 130 cosmic rays, and 3) charged particle dynamics in Earth's Van Allen radiation belts. In
 131 all these cases, it is critical to measure not only energy spectra, but also to identify par-
 132 ticle species. For example, to fully understand SEP energization, identification of par-
 133 ticle species and charge states is of utmost importance (Reames, 2020). While the sci-
 134 ence objectives are described in detail (Section 2.1 through Section 2.5), an overall sum-
 135 mary is provided by the science traceability matrix in Table 1. Note that the traceabil-
 136 ity matrix refers to the full version of AGILE and not to the prototype that will fly on
 137 GenSat-1 (see Section 7). The chief difference between the two is the number of detec-
 138 tor layers (16 for the full version and 3 for the prototype). The front end electronics, and
 139 the fast sampler chip are anticipated to be the same for both the prototype and the full
 140 version of the instrument, albeit with modified gain settings to optimize both electron
 141 and ion characterization.

142

2.1 Solar Energetic Particles

143

144

145

146

147

148

149

150

151

152

153

154

155

156

AGILE is capable of addressing unanswered questions on the topic of the energization of solar energetic particles (SEPs), which is currently not fully understood (Desai & Giacalone, 2016). For example, the relative contribution from shocks associated with coronal mass ejections (CMEs) and corotating interaction regions (CIRs) has not been determined. Additionally, the respective dynamics of impulsive (^3He -rich) and gradual (proton-rich, average Fe/O ratios ~ 0.1) events have not been untangled (Desai and Giacalone (2016) and references therein). Further complicating matters, SEPs overlap in species and energy with ACRs (for a review, see Reames (1999)). As a result, separating the two, and subsequently probing the dynamics of SEPs, is challenging. Measurement of elemental abundances in SEP events is important to help establish the nature of SEP energization (Reames, 2020). AGILE's first science objective is to resolve ion mass (Gautier et al., 2021) and measure the relative abundance of various isotopes. AGILE will be capable of separating both ion species and isotopes to address SEP science topics.

157

2.2 Anomalous Cosmic Rays

158

159

160

161

162

163

164

165

166

167

168

169

170

171

172

173

174

The modulation and generation of Anomalous Cosmic Rays (ACRs) (for a review, see B. Klecker (1999)) is another important science question that is poorly understood. Previous measurements of ions in the Earth's outer radiation belt have shown that ACRs with sufficient rigidity can penetrate Earth's magnetosphere and get trapped in the radiation belts (see for example, Scholer (1975)). Measurements by the SAMPEX satellite in high inclination LEO have characterized these trapped populations as well as their solar cycle dependence (Cummings et al., 1993; Selesnick et al., 1995). More recently, R. Leske et al. (2013) reported on an unusual discrepancy between ACR and GCR intensities during solar cycle 23/24 which may shed light on the modulation and generation of ACRs. Thus, the study of ACRs and their trapping in the magnetosphere are of significant importance in the study of heliospheric charged particle dynamics. Figure 1 shows an artist's rendition of SAMPEX observations of trapped ACRs, complementing the well-known inner and outer belts. Nearly twenty years prior to these observations, Blake and Friesen (1977) predicted ACR trapping. However, direct observation of these trapped ions is challenging due to the difficulty of accurately determining particle species and energy. AGILE as a science payload in high inclination LEO can measure trapped ACRs and on an interplanetary platform study their modulation and transport from the distant heliosphere.

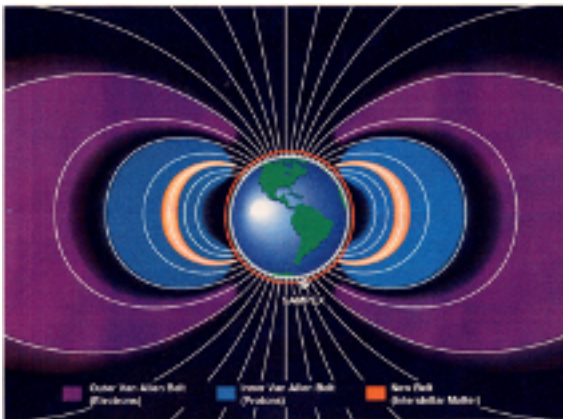


Figure 1. SAMPEX observes trapped ACR (shown in orange). The outer Van Allen belt is shown in purple, while the inner belt is in blue.

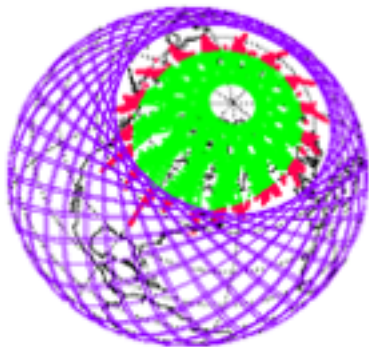


Figure 2. SEP ions can reach the ISS during disturbed times. Purple lines show the ISS ground tracks, and the green area is the nominal polar cap. Areas that overlap with the space station are shown in red.

175

2.3 Space Weather

176

177

178

179

180

181

182

183

184

185

186

187

188

189

190

It is well known that there is a significant risk to space-based assets during significant solar and geomagnetic activity (Baker et al., 2018). Aircraft communication can be disrupted with increased energy input from precipitating heliospheric particles. Spacecraft electronics are sensitive to energetic electron and ion fluxes via dielectric charging and single-event upsets, respectively. Additionally, humans outside of Earth’s atmosphere can be subjected to adverse doses of radiation. It is well known, for example, that energetic ions can reach the International Space Station (ISS) orbits during intense geomagnetic storms (R. A. Leske et al., 2001) and pose serious radiation hazard to astronauts during extravehicular activity (EVA). Figure 2 shows the location of >16 MeV Oxygen during the Oct-Nov, 1992 SEP events. Solid lines are ISS ground tracks and the green area is the nominal polar cap. It is evident that there are times when these heavy ions can overlap with the region of the space station (red), increasing the space weather risk of human activity in space. AGILE is capable of identifying and monitoring hazardous particle populations, and their increased access to low altitudes, during geomagnetically disturbed times.

191

2.4 Inner belt energetic electrons

192

193

194

195

196

197

198

199

200

201

202

It is extremely difficult to measure electrons in the inner zone due to the overwhelming presence of energetic protons, which penetrate through the instrument shielding and overwhelm the electron signal (for recent observations, see Fennell et al. (2014); Li et al. (2015); Turner et al. (2017)). As a result, detailed and reliable observations of electron dynamics in the inner zone have not been made for the simple reason that it is extremely challenging to separate coexistent electron and proton populations. AGILE’s pulse shape discrimination allows for accurate particle characterization, including energy and species information and will thus, with great reliability, remove proton contamination from electron measurements. AGILE will directly address the outstanding question of the presence or absence of energetic (>1 MeV) electrons in the inner belt and characterize their dynamics.

2.5 Outer belt electrons

While the current version of AGILE to be flown on GenSat-1 (see Section 7) will focus primarily on ions, a planned future version of AGILE will additionally measure electrons from $< 1\text{MeV}$ to $\sim 10\text{MeV}$ and provide the capability to observe both seed ($< 100\text{s}$ of keV) and accelerated ($> 1\text{MeV}$) populations of Earth's outer radiation belt electrons. Simultaneous measurements of these populations are necessary to understand the unanswered processes behind relativistic electron acceleration (Baker et al., 2016; Kanekal et al., 2015; Jaynes et al., 2015). Various studies explain that the outer belt electron acceleration is caused predominantly by inward transport due to Ultra-Low Frequency (ULF) wave activity (Mann et al., 2016), or exclusively by local acceleration caused by Very-Low Frequency (VLF) wave activity (Reeves et al., 2013). Yet other studies show that neither is sufficient; both are needed to produce MeV electron enhancements (Kanekal et al., 2015; Zhao et al., 2018). Separating the relative contribution of local energization and radial transport is critical to understand the dynamics for each event. For example, observing an enhancement in the energized population without the presence of a seed population will unambiguously determine radial transport as the energization mechanism. The planned future version of AGILE will provide clean electron measurements and help probe electron acceleration, transport, loss processes in the outer zone.

2.6 Science Closure

AGILE will directly address the SEP and ACR, space weather aspects, and outer belt electron science goals. It will do so with robust and reliable identification of particle species and by measuring their energy spectra using pulse shape discrimination, for the first time in space. AGILE's unique ability to distinguish particle species can provide a window into regimes where simultaneous measurements of different populations had previously prevented identification. Specifically, AGILE can measure and distinguish ion species, from H to Fe, in addition to their isotopes. Simultaneous measurement of incident energy directly closes Science Goal (1) to study the energization of SEPs and the dynamics of ACRs. AGILE can also accurately measure proton and ion spectra to characterize SEP access to high-latitude regions, as well as particle penetration to low latitudes during geomagnetically active times. These measurements directly address Science Goal (2) to study the effects of interplanetary particles on human activity in space. Additionally, AGILE is the first instrument capable of simultaneously and accurately measuring energetic electron dynamics in both the inner and outer radiation belts. AGILE's on-board pulse discrimination will provide reliable particle species identification, allowing for the separation of energetic electrons from the overwhelming proton signal in the inner belt. Additionally, AGILE is capable of measuring the wide range of electron energies that is required to probe the dynamics of accelerating outer belt electrons to relativistic energies. These measurements directly close Science Goal (3) to study the dynamics of energetic electrons in both of Earth's radiation belts. These science objectives can be achieved with reliable identification of species, isotope, and energy of incident particles, which is done with the unique pulse shape discrimination method.

3 Particle Identification by pulse shape discrimination

As discussed in Section 1, identifying charged particle species is necessary to advance our understanding of energization, transport, and loss from the sun and terrestrial magnetosphere to interplanetary space. Traditional methods using particle telescopes relied on the ΔE -E method, i.e., using patterns of energy deposition in detectors (e.g. solid-state detectors) and have been used in space physics for a long time, for example particle detectors on Voyager (Stilwell et al., 1979; Stone et al., 1977). Ammerlaan et al. (1963) provided the theoretical description of pulse shape dependence upon particle type and experimentally validated the particle ID capability. In addition, Ammerlaan

et al. (1963) pointed out that the PSD method can be used with a single detector and emphasize the advantage of PSD, namely the avoidance of using very thin detectors to reduce electronic noise. The feasibility and applicability of the PSD method have been demonstrated on ground based detection systems (Carboni et al., 2012). However, it is the recent advances in fast electronics that have enabled the applicability of PSD to space based instrumentation through the development of very high (ps) time resolution low-power ASICs.

3.1 Principles of pulse shape discrimination (PSD)

In a particle telescope configuration, ions with varying kinetic energy stop at different depths in the detector stack. They can be identified using the pulse shapes only from the deepest detector impacted, thus enabling identification of low energy ions at the front of the stack and the highest energy ions from the detectors deeper in the stack. The PSD method also enables detector energy thresholds to be set lower (Gautier et al., 2021; Carboni et al., 2012) as compared to the $\Delta E-E$ technique because the latter requires thinner detectors, prone to energy straggling, electronic noise, and mechanical failures, to achieve similar low-energy resolution.

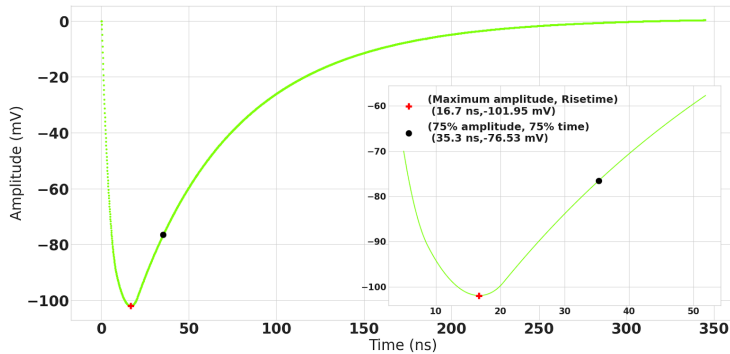


Figure 3. Simulated signal in the stopping layer of a stack of three Si detectors, each 300 microns thick. In this instance, the signal is produced by a 20 MeV/n Oxygen ion stopping in the second layer. The inset shows a zoomed-in view with the legend stating the numerical values of rise time and amplitude values.

268

The AGILE approach is based upon measuring two key characteristics of each pulse produced by a particle stopping in the detector (after an amplifier chain), termed the "Rise Time" and the "Maximum Amplitude". An example of these characteristics, obtained using detailed simulations (see Gautier et al. (2021)), is illustrated in Figure 3, which shows the signal generated by an Oxygen ion of 20 MeV/n in a Si detector 300 microns thick. Figure 3 shows that the rise time of the generated pulse is on the order of 17 ns, and the inset indicates the key characteristics used for PSD. Therefore, in order to accurately determine this time, a fast sampler is required. AGILE achieves this using the recently developed PSEC4 custom ASIC (Oberla et al., 2014). The details of the PSEC4 ASIC are described in Section 4.3.

These key characteristics of amplitude and rise time are unique for different species of ions stopping in a given detector. The AGILE collaboration has recently shown, using high-precision simulations, (Gautier et al., 2021) that various ion species can be clearly discriminated using the PSD technique. Figure 4 reproduced from Gautier et al. (2021) shows the tracks of various ions ranging from $Z=2$ to $Z=26$ obtained in a single Si de-

283

284

tector. Clear separation of the "tracks" is evident for ions from He to Fe in the energy range spanning 3-6 MeV/n (He) and 12-22 MeV/n (Fe).

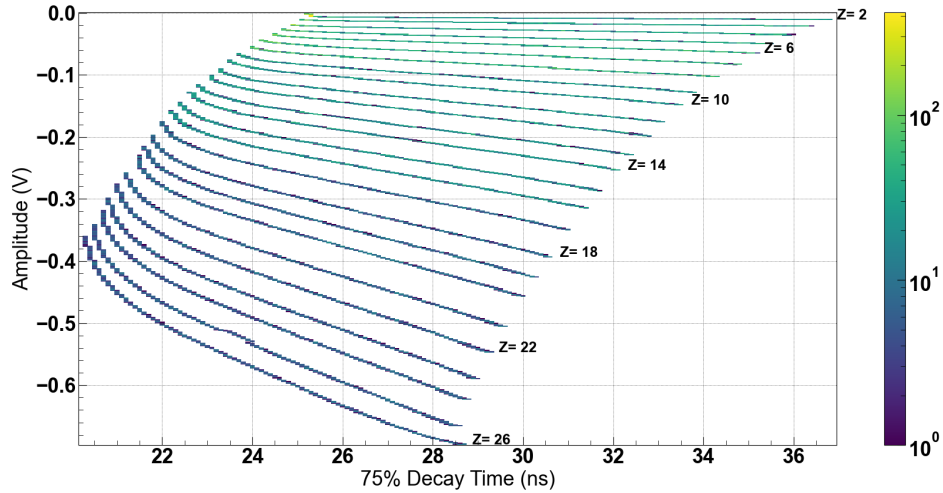


Figure 4. He to Fe ($Z=2$ to 26) tracks of maximum amplitude vs rise time in the stopping layer. The tracks are well separated for each species over the full simulated energy range (3-6 MeV for He and 12-22 MeV/n for Fe) of the incident ion. Color bar to the right shows the number of particles in each energy bin. Particle ID is obtained from its characteristic track, and its energy from the amplitude (Gautier et al., 2021).

285

286 4 AGILE implementation

287 The AGILE instrument comprises front end electronics (FEE) cards with on-board
 288 solid state detectors (SSD) (Section 4.1), a power supply board to bias the SSDs (Sec-
 289 tion 4.2), the PSEC4 chip (Section 4.3) on the controller board (Section 4.4). The anal-
 290 og signals are connected to the controller board by coaxial cables, and the digital con-
 291 nectivity is provided by the backplane, to which the power, FEE, and controller boards
 292 mate via connectors. Table 2 lists the instrument performance requirements. A struc-
 293 tural block diagram of the instrument, slated to fly on GenSat-1 (Section 7) in Fall 2022
 294 is shown in Figure 5.

295 The SSDs are arranged in a stacked disc configuration and are 20mm in diameter
 296 and 300 microns thick. For GenSat-1, the AGILE instrument comprises three SSDs in
 297 order to fit in a $\approx 1U$ form factor. AGILE communicates to the S/C and receives power
 298 through a connector at the side. Once an ion travels through the detector stack, the sig-
 299 nals are processed by fast analog read-out electronics and fed into a fast high-resolution
 300 sampler. This allows for the main signal characteristics to be obtained. The Teensy mi-
 301 crocontroller extracts relevant characteristics of incoming signals to generate compact
 302 data products used for later discrimination of the particles ID and their energy. Figure 6
 303 illustrates the concept showing a high level functional block diagram of AGILE.

304 The AGILE structure housing the component subsystems is a rectangular box with
 305 the outer housing being made of Al with a tungsten plate placed behind the front Al layer.
 306 An inner tungsten tube lines Al tube that sets the instrument aperture. Both the tung-
 307 sten plate and the tube are 1mm thick, and serve to reduce bremsstrahlung background
 308 (Kaneval et al., 2019). A window comprising two layers of aluminized kapton, each 8 mi-

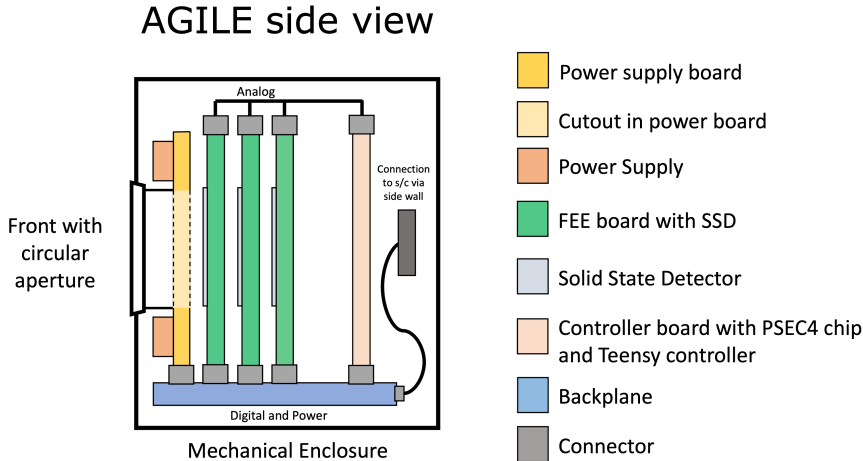


Figure 5. AGILE schematic illustrating the instrument concept. The figure is a side view of AGILE showing the front end electronics cards with SSDs, bias power supply, redundant Teensy controller board with PSEC4 chip. All these boards connect to a backplane which carries various digital data as well as bias power to the detectors. Analog signals from the detectors are sent to the controller board via harness shown at the top. A connector on the side connects to the S/C bus via a separate harness (not shown).

Table 2. Instrument Performance & Resources

Measurements and Functional Parameters	
Ions	$\approx 2\text{-}100 \text{ MeV/nuc}$
Energy Resolution	30%
Sampling Rate	4-15 GSa/s
Geometry Factor	$0.61 \text{ cm}^2 \text{ sr}$
Mass	$< 1 \text{ kg}$
Resource Parameters	
Power	1.6W (orbit avg.)
Data rate	0.209 - 834 kbps

309 crons thick, serve to block light. The bevelled opening determines the geometry factor
 310 and has a value of $0.61 \text{ cm}^2\text{-sr}$. A CAD drawing of the instrument is shown in Figure 7.
 311 The aperture is at the top of the image, with the three SSD shown as gray circles on the
 312 first three boards below.

313 4.1 Solid State Detectors (SSD) and Front end electronics (FEE)

314 The SSDs for AGILE are $300 \mu\text{m}$ thick silicon sensors. They are ion implanted P-
 315 type bulk silicon with full metallization on both active and ohmic sides with a dead layer
 316 of $0.3\text{-}0.5 \mu\text{m}$, with Aluminum metallization $0.3 \mu\text{m}$ thick. These thicknesses correspond
 317 to electron (proton) thresholds of 4 keV (90keV), which are far below the lowest ener-
 318 gies to be measured by AGILE. Figure 8 shows the SSDs used for AGILE. The active
 319 area of the detector is surrounded by a multi guard ring (MGR). The MGR is a series
 320 of implanted and metallized rings that surround the active area and allow a potential
 321 drop from the inner ring closest to the active area to the outermost ring. Wire bonding

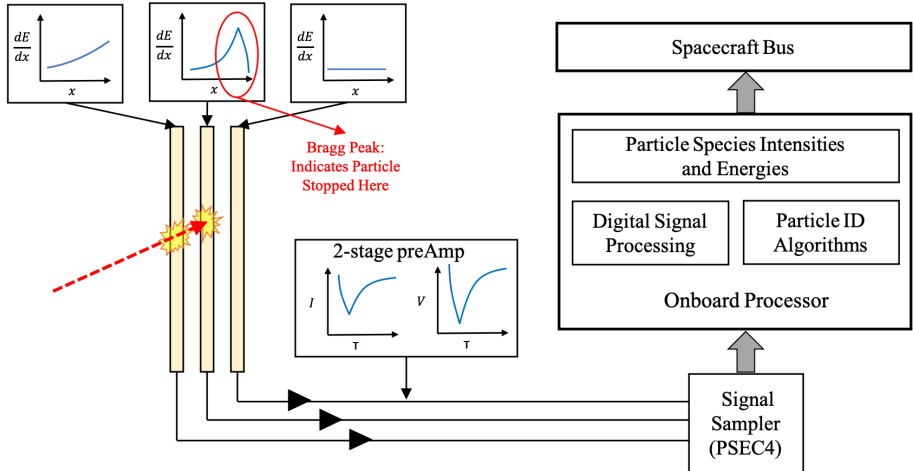


Figure 6. Simplified schematic of PSD method (3 layer configuration): a particle stops in the second detector (Bragg peak) while passing through the first with no signal measured in the third detector. The signals from each detector are processed by fast analog read-out electronics and fed into a fast high-resolution sampler (PSEC4), which digitizes the entire signal from each detector layer. The Teensy controller processes the sampler output and transmits the data to the main processor on the spacecraft.

connections are made to the innermost MGR and biased to the same potential as the active area. A proprietary feature of the detectors includes the so-called field plate (FP). The FP is an isolated metal boundary on the front junction side that fills the region from beyond the last outer MGR to just before the chip edge. The FP is biased to the same potential as the rear ohmic side of the chip internal via a through plated hole. Laboratory tests have shown that the FP biasing improves the stability of the chips and extend the breakdown voltage.

The front end electronics (FEE) processes the current signals from the sensor and generates voltage output signals with an amplitude proportional to the energy deposited by the electrons and ions. The AGILE instrument covers a very wide variety of charged particles and energies, the range of signals produced by incoming particles in the Si detector is about $10^{-7}A$ to $10^{-2}A$, i.e., covers about 5 orders of magnitude. In order to address this and to optimize the output for the downstream digitizer (see section 4.3), the FEE has two analog outputs: a single stage low gain output and an high gain output after 2 additional amplification stages. The entire amplifier chain is designed to maintain the shape of the sensor signal with high fidelity so that the information contained can be used for particle identification. A block diagram of the 3-stage amplifier is shown in Figure 9.

The block diagram of the FEE is shown in Figure 9, and the output signals measured with an Alpha source (Am-241) in Figure 10. For ions with low incident energy, as in this case (AM241 alphas have a total energy of ~ 5.2 MeV) the output from the high gain stage is the relevant one. Figure 10 bottom panel shows the raw signal output from the high-gain amplifier to be clean with little noise.

The SSDs are supplied by Micron Semiconductors, LLC, UK, and are mounted directly on the FEE boards. A photo of the assembled FEE engineering model (EM) board together with a SSD is shown in Figure 11. The EM board will be used for calibration and characterization in the laboratory. The figure shows a 300 micron thick detector on the left side of the board with the FEE on the right. For the flight model (FM) the FEE

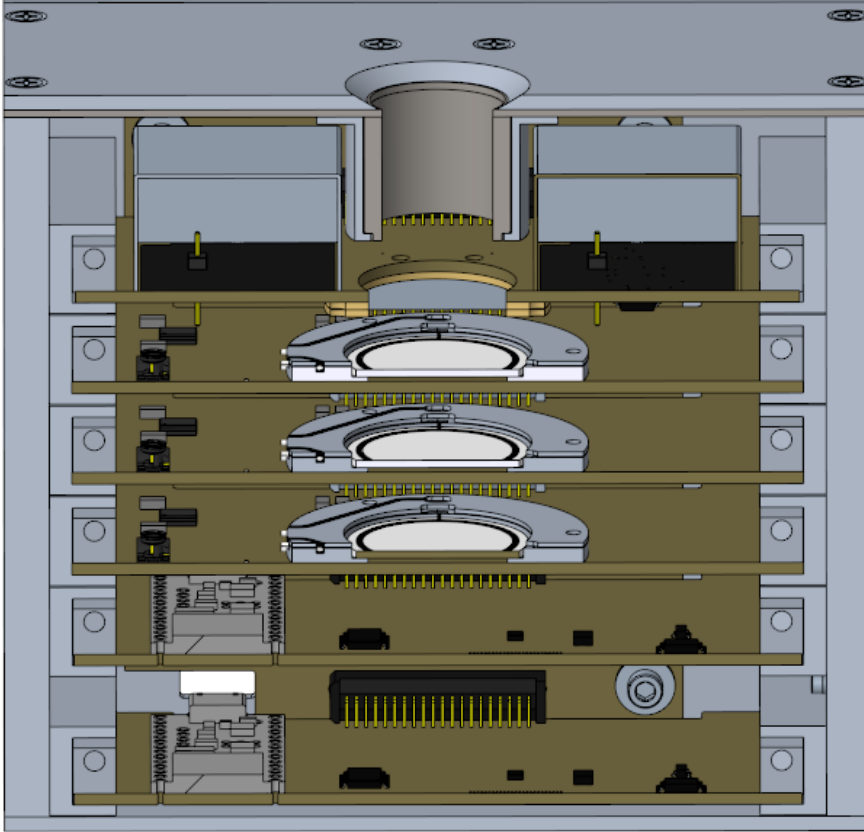


Figure 7. CAD drawing of the AGILE instrument

350 boards will connect to a "backplane" via an MDM connector. The backplane will provide
 351 digital connectivity between the FEE, the PSEC4 chip (Section 4.3) and Teensy on
 352 the controller board. After the signal is amplified by the FEE, the analog signals are dig-
 353 itized and sampled by the PSEC4 chip, which digitally samples the waveform of each ana-
 354 log signal for particle identification.

355 4.2 Bias Power supply

356 The detectors are biased using a CAEN A7508 power supply (<https://www.caen.it/products/a7508/>).
 357 There are two power supplies located on the board directly behind the instrument face.
 358 The board also contains two aluminized Kapton foils in order to limit low energy parti-
 359 cles (<1MeV) from striking the SSDs. Each supply takes 5V input and supplies the
 360 bias voltage ($\sim 100V$) to the detector boards via the backplane. The bias voltage is ad-
 361 justable in a linear fashion via an applied voltage (V_{set}) which has a voltage range of 0
 362 to 2V. The control and monitoring of the power supplies are carried out by onboard mi-
 363 crocontroller (section 4.4) as well as two sets of digital-to- analog converters (to set the
 364 bias voltage) analog-to-digital converters (to monitor the output voltages and currents).
 365 Only one power supply will be used at a time to power the detectors with the second pro-
 366 viding redundancy in case of failure. The power supply board has a thermistor to mon-
 367 itor the temperature, which is also available to the microcontroller and reported as part
 368 of house keeping (HK) data.

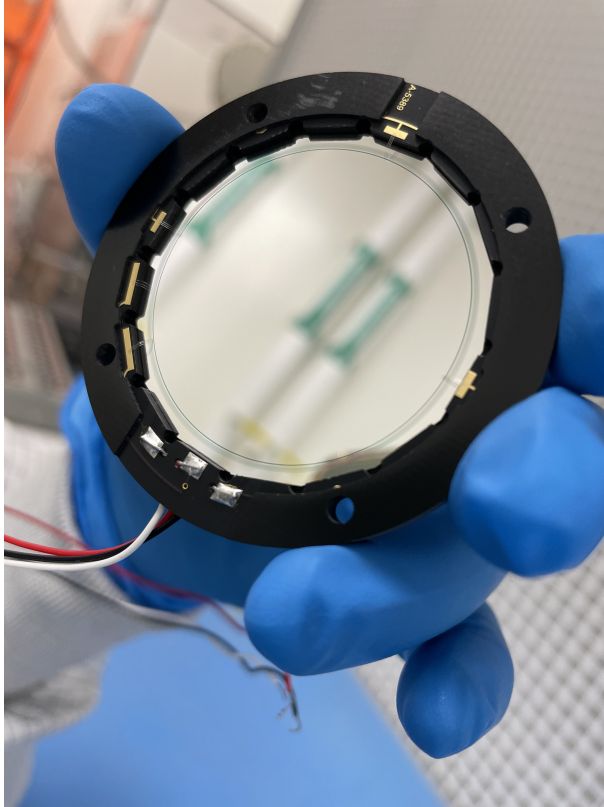


Figure 8. A photo of one AGILE SSD showing the packaging and the active (black), ohmic(red) and the guard ring (white) connections. Clockwise from the bottom left white/black/red wires, the Field Plate and the Multi Guard Ring and the active are connections are shown. All connections are triple bonded for redundancy.

369

4.3 Pulse shape measurement using PSEC4 ASIC

370

371

372

373

374

375

Switched capacitor arrays (SCAs) are frequently used to record snapshots of transient waveforms, i.e., pulses, because they can sample a limited time-window at a relatively high rate, but with a latency cost of a slower readout speed (Haller & Wooley, 1994). They are used most frequently in high-energy physics, but are not commonly used for space-based applications. Modern circuit design allows for SCA chips to be compact, low power, and relatively low cost per channel (Kleinfelder, 1988).

376

377

378

379

380

381

382

383

384

The PSEC4 is a custom integrated circuit to record fast waveforms. On each of the 6 analog channels, the PSEC4 has an SCA with 256 samples. The sampling rate can be adjusted between 4 GSa/s and 15 GSa/s. PSEC4 offers a fast, robust and low-power waveform sampling. AGILE is currently designed to operate at 5 GSa/sec although can go up to 10 GSa/s if needed. These characteristics make it very capable for space-based detection of full wave form resolution of discrete high-energy particles. The fast sampling characteristic is primordial for the full digitalization of the rising-edge of signals (which are on the order of 10 ns). Trigger discriminator in each PSEC4 channels allows flexibility in the instrument configuration. Figure 12 shows a photograph of the PSEC4 chip.

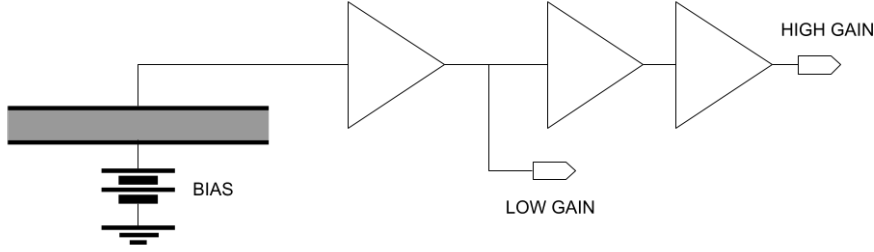


Figure 9. Block diagram of the triple stage amplifier. The FEE is designed to work with PSEC4 sampler ASIC. Therefore, the two output signals are always below 1V and at least one of the two will have a signal of 10 mV for the particles with very low ionization.

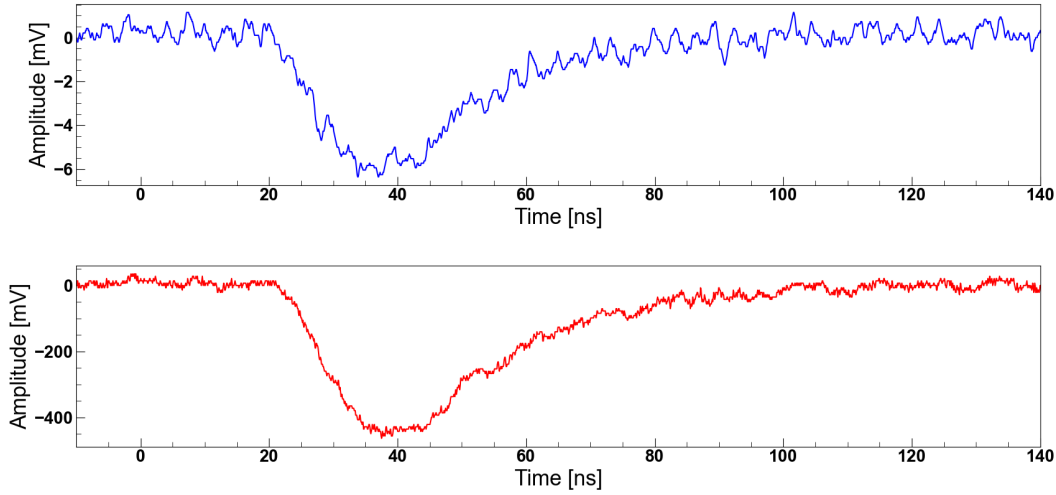


Figure 10. Voltage output from the FFE amplifier as a function of time in response to an alpha particle. Top panel shows the low gain and bottom panel shows high gain raw output.

385

4.4 Controller Board

386

387

388

389

390

391

392

393

394

395

396

397

398

The PSD output from the the PSEC4 comprises 256 samples of the waveform for each particle and each detector, resulting in a very large data volume (with even a byte per sample). This is clearly impractical to telemeter down, especially for CubeSats. However, particles that stop in the detector stack can be identified by measuring only the rise time and amplitude of the signal, as has been demonstrated by Gautier et al. (2021). An onboard microcontroller performs the processing of this raw data for storage and subsequent download to Earth. The microcontroller is also in charge of the control of other components such as the PSEC4 readout and communication through SPI interface with the spacecraft. The controller used for AGILE is the Teensy 4.1 (Stoffregen & Coon, 2014) which uses an ARM Cortex-M7 microcontroller at 600 MHz and provides 8 MB of internal memory with capability to extend up to 16MB additional PSRAM memory. The choice of Teensy 4.1 was dictated by its compactness and its low power consumption compared to great computational power.

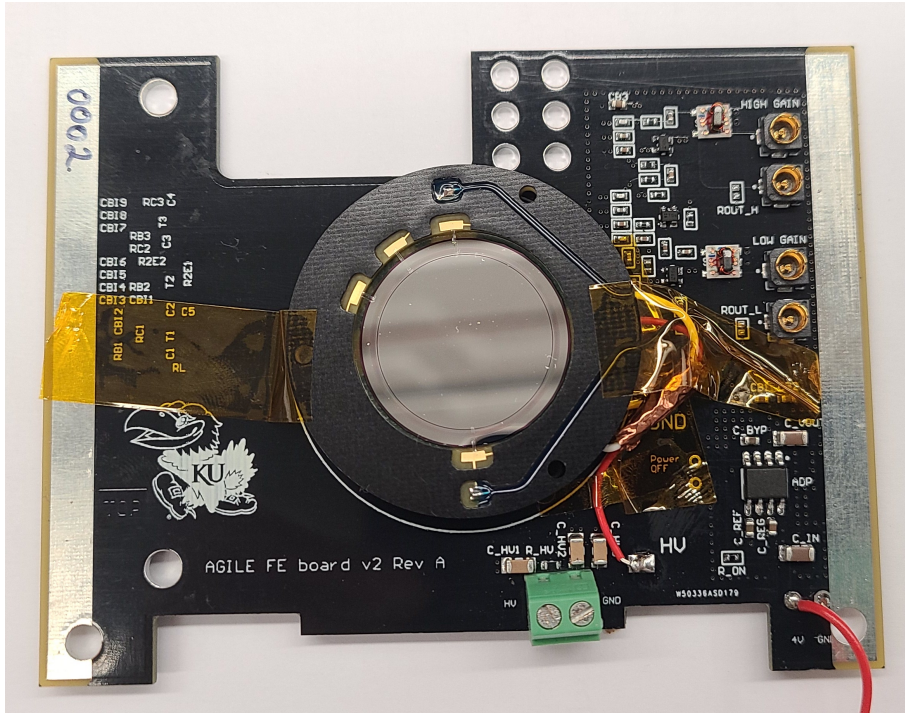


Figure 11. A photo of the assembled FEE board together with a SSD.

399 Figure 13 shows a simplified diagram of the controller board operation. Each of
 400 the 6 PSEC4 channels has trigger discriminators providing individual trigger (self-trigger)
 401 bits depending on the pre-defined threshold levels. Then these self-triggers are processed
 402 by the on-board CPLD (Complex Programmable Logic Device) or FPGA (Field-
 403 Programmable Gate Array) and depending on the trigger strategy (e.g. coincidence of 2 chan-
 404 nels) the "global trigger" is generated and the analog signals from the FEEs are digi-
 405 tized and stored in the controller board memory of 8MB currently and is upgradeable
 406 to 16 MB. In order to handle the trigger logic based on a predefined trigger mode and
 407 individual "self-triggers" of the PSEC4 chip and to produce the "global trigger" (a sig-
 408 nal at which the analog signals from the FEEs will be digitized and stored) a CPLD is
 409 used. A simplified diagram of the controller board operation is shown in Figure 13.

410 4.5 Backplane

411 The backplane is used as an interface between the three FEE cards with the power
 412 and controller cards, as well as to provide the data to the spacecraft. The interface to
 413 the spacecraft harness is AGILE's only connection to the outside world. There are 45
 414 pins required for internal components and 15 to connect to the harness, which include
 415 power to the instrument and communication protocol channels. A heartbeat signal will
 416 pass through the backplane to check for Teensy aliveness.

417 5 Calibration and Testing

418 Currently the approach being considered for determining particle type and energy
 419 is based on using simulated interactions of particles in silicon using Geant4 (Agostinelli,
 420 2003) and WEIGHTFIELD (Cenna et al., 2015) models. The AGILE collaboration has
 421 performed detailed simulations (Gautier et al., 2021) and measurements using radioac-
 422 tive source confirming the reliability of the approach.

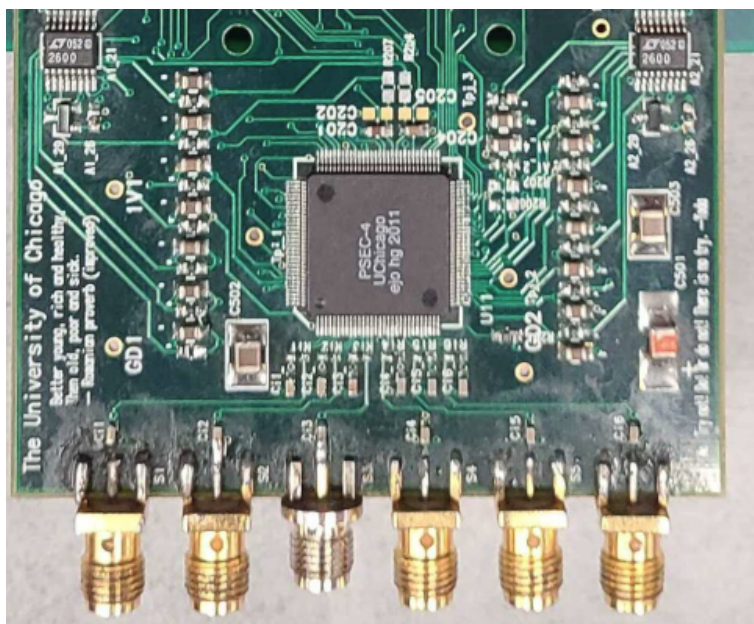


Figure 12. Photograph of a PSEC4 test board. The PSEC4 chip can be seen at the center of the board.

423 The AGILE instrument will be calibrated at the component (i.e., detector) level
 424 as well as at the instrument level. For the upcoming GenSat-1 mission, a 4 cycle ther-
 425 mal vacuum (TVAC) test and a vibration test as prescribed by the launch vehicle require-
 426 ments will be conducted at the spacecraft level. Prior to TVAC and vibration tests, an
 427 instrument-level calibration using accelerator beams will be carried out. The fully as-
 428 sembled instrument will be exposed to ion beams of differing energies at the NASA Space
 429 Radiation Laboratory (NSRL) facility located at the Brookhaven National Laboratory
 430 (BNL). This facility can provide ions from He to Fe in the energy range from stopping
 431 to 1500 MeV/n, which covers the AGILE energy range. The team is currently schedul-
 432 ing beam time at NSRL and BNL.

433 6 AGILE data products and operational modes

434 As discussed in previous sections, particles of different species, masses, and ener-
 435 gies interact with the solid state detector differently. A snapshot of how the charge is
 436 deposited in the detector contains information about the incident particle. AGILE’s dig-
 437 ital signal processing is fast enough to capture that interaction.

438 This section describes how AGILE directly transfers information into a data packet
 439 (Section 6.1), and how AGILE processes the data for a reduction in volume (Section 6.2).
 440 AGILE has two modes of data collection, namely the full waveform mode and the key
 441 features mode. These modes are switchable by ground command and are described be-
 442 low.

443 6.1 Full Waveform Mode

444 A particle impacting a detector leads to two waveforms from the low- and high-
 445 amplifier chains with the complete waveform containing 256 samples. If a particle reg-
 446 isters a hit on all three detectors, the six waveforms generated produce 1536 points that
 447 are used to identify the particle. This is the first of the two AGILE data products, namely,

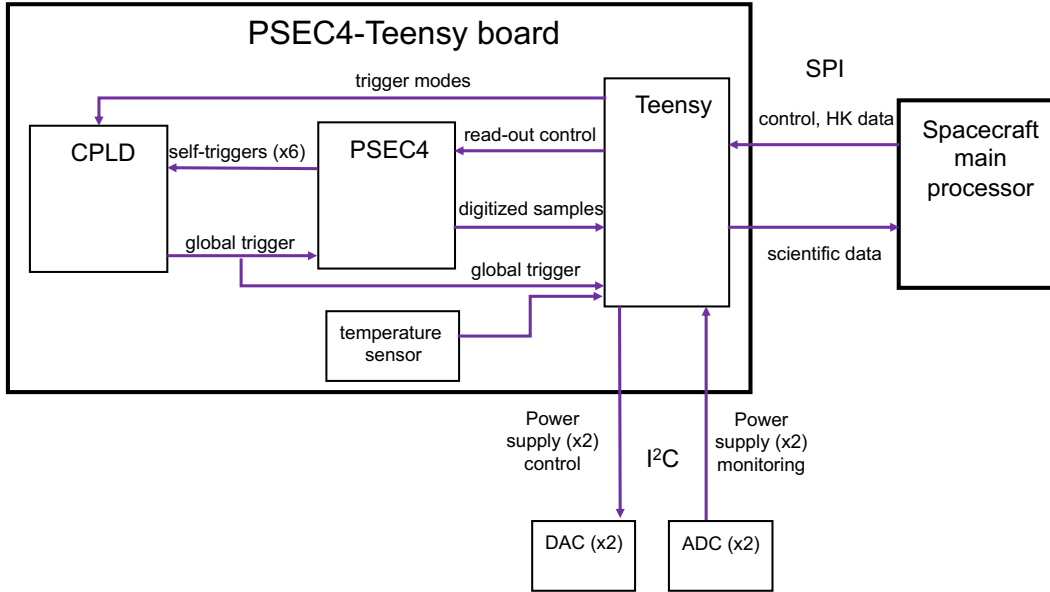


Figure 13. Block diagram illustrating the Teensy controller operation. The PSEC4 samples the amplified signals from the detectors resulting from particle passage. The digitized samples (PSD) acquired as per pre-loaded triggers (see text) are passed on to the Teensy. The sampled data are stored on Teensy and particle key parameters are extracted (see text) from the full PSD samples. The Teensy also monitors AGILE temperatures via two thermistors, located on the power supply and micro-controller boards respectively.

448 the full waveform data. This data product is a recording of the raw output of each de-
 449 tector for each registered hit event. However, each of the 1536 words uses 12 bits, result-
 450 ing in 18.4 kbits of information for a single event. For periods of high flux, the data gen-
 451 eration rate becomes a limiting factor of the information that can be transcribed for each
 452 event. Despite some possible compression, the key features mode, described below, is pre-
 453 ferred during high flux periods to reduce data rate.

454 6.2 Key Features Mode

455 Detailed simulations (Gautier et al., 2021) have shown that each incident particle
 456 can be identified using only 2 values: the signal rise time and the signal maximum am-
 457 plitude. The onboard processor, Teensy, will perform an algorithmic determination as
 458 follows: The first step will retrieve the signal from the layer where the particle stopped.
 459 The signal would then be characterized for maximum amplitude and rise time. To in-
 460 crease the reliability and provide redundancy, AGILE’s key parameter mode uses 10 key
 461 values: 5 samples of waveform amplitude and their corresponding times. The specific time/amplitude
 462 data that is recorded is determined using simulations described in Gautier et al. (2021).
 463 Thus, this mode reduces the data generation rate from 1536 words/event to 10 words/event.

464 6.3 Priority based processing

465 AGILE data processing includes ability to prioritize type of data collection using
 466 signal (i.e., energy deposited in the detector) threshold levels. The threshold required
 467 to record a signal will set the level of energy deposition above which the data will be sam-
 468 pled by PSEC4. A low energy threshold results in higher number incident particles to
 469 be advanced through the signal chain, as well as accept heavier ions. This will directly

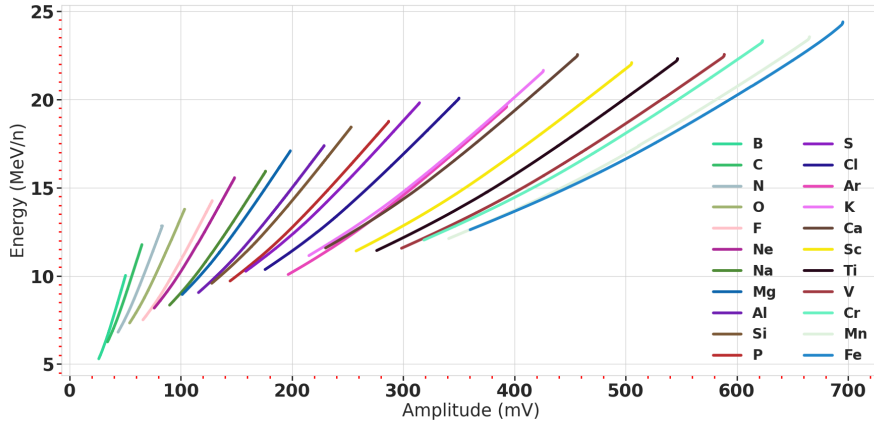


Figure 14. Estimated energy as a function of measured Maximum amplitude in layer 1 when the identification of particle ID is possible (Gautier et al., 2021).

470 influence the number of events recorded and processed by AGILE. Since SEP energy spec-
 471 tra are usually falling (e.g., Reames (2020)), a lower threshold will result in exponentially
 472 higher count rates. Conversely, a higher threshold not only reduces the expected count
 473 rate, but also selectively increases the ratio of heavier ions observed in the data.

474 Priority based data processing will be performed onboard via stored procedures.
 475 The method to determine particle ID and its energy will be encoded in Teensy and fol-
 476 lows previous key features extraction. These characteristics will then be compared to sim-
 477 ulated values to identify particle species. This comparison would be via a lookup table
 478 based on simulation and beam test results. A second lookup table will be used to de-
 479 termine the particle energy. Figure 14 shows the lookup table in the form of a plot that
 480 would be stored on Teensy to perform the energy measurement. The full details of the
 481 simulation are discussed in a paper by the AGILE collaboration (Gautier et al., 2021).
 482 The simulation provides estimates of uncertainties associated with the assigned energy.
 483 Ambiguous or multiple identities and energies for a given event would be retained and
 484 telemetered down to ground for further detailed analysis.

485 7 AGILE in Space: GenSat-1

486 AGILE will be part of the science payload on a CubeSat platform, the GenSat-1
 487 being built by Genesis systems at their facility in Lanham, MD. Gensat-1 is 6U Cube-
 488 Sat and will fly in a high inclination LEO at 500 km altitude. AGILE will be oriented
 489 with its field of view (FoV) within a few degrees of the local zenith (the actual devia-
 490 tion to be determined from attitude control characteristics). AGILE has a FoV of $\approx 56^\circ$
 491 and therefore does not require high pointing accuracy. This is ideal to observe SEP over
 492 the polar cap regions as well as the terrestrial radiation belts.

493 GenSat-1 is expected to launch fall 2022 with an expected delivery date for AG-
 494 ILE being early 2022. The spacecraft provider will integrate the AGILE payload and be
 495 responsible for data downlink as well as commanding uploads (C&DH). The GenSat-1
 496 science mission will be of one year duration and therefore expected to observe multiple
 497 SEP events and hundreds of passes through the radiation belts.

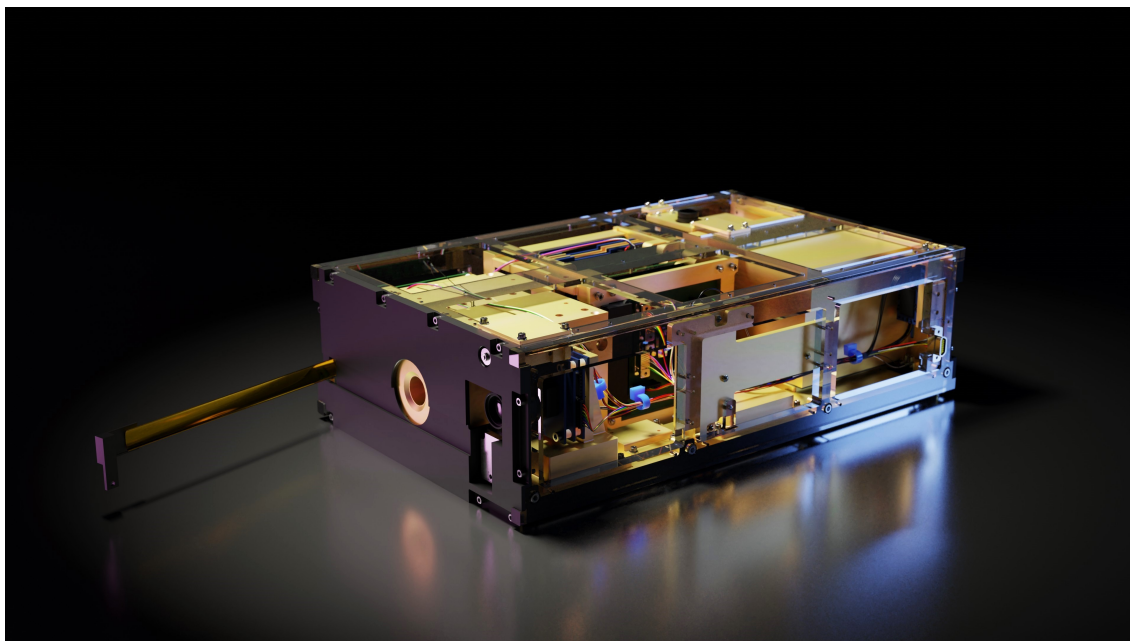


Figure 15. The GenSat-1 CubeSat showing AGILE payload’s circular aperture on the front face. GenSat-1 will be in high inclination LEO with AGILE looking zenith-wards over the Earth’s polar regions

498

8 Summary and Conclusions

499

500

501

502

503

504

505

506

507

508

509

510

511

512

513

514

515

In this paper, we have described AGILE, an innovative instrument to determine particle species and energies using full pulse shape discrimination (Gautier et al., 2021) for the first time in space-based instrumentation. AGILE uses the state-of-the-art technology of fast pulse sampling (pulse shape discrimination, PSD) of a few pico-seconds enabling full characterization of charge pulses from solid state detectors which are usually 10s of nanoseconds long. A multi-stage charge sensitive amplifier preserving the information contained in the pulse originating from particle passage through the detector ensures PSD based particle ID and energy determination. The AGILE team has carried out detailed end-to-end simulation of particle passage through detectors (Silicon) including signal generation and electronics response. Full details of the simulation are described in Gautier et al. (2021). Two outstanding features of the PSD approach deserve reemphasis, i.e., ability to measure ions at a lower energy thresholds without complications (e.g., noise) arising from using thin detectors in the traditional ΔE -E method, and obtaining particle ID from the signal induced in a single detector. While the PSD method has been used in ground-based experiments for a long time (Ammerlaan et al., 1963), it is the recent advent of innovative low power ASICs that has enabled the applicability of the PSD technique in space.

516

517

518

519

520

521

522

523

AGILE on GenSat-1 will primarily focus on measuring SEP, trapped ACR ions and secondarily on radiation belt electrons. However, while this prototype has not been optimized for measuring electrons, the complete version with sixteen detectors instead of three will address relativistic electron dynamics in the terrestrial radiation belts. The full version of AGILE will help address outstanding issues in our understanding of energization and transport of SEP, dynamics and trapping of ACRS, and the vexing question of unambiguously characterizing electrons in the proton dominated inner radiation belt. The complete version of AGILE will be fully calibrated at accelerator beams,

524 such the NASA facility at Brookhaven National Laboratory (BNL). The AGILE team
 525 is in contact with the beam providers and has defined a test plan encompassing most SE-
 526 Pion species and covering the energy range requirements. The team has also ascertained
 527 that the BNL facility can provide single particle per pulse (statistically speaking) which
 528 is required for absolute energy and species calibration.

529 The compact and low power nature of AGILE makes it highly appropriate solu-
 530 tion for constellation and formation type multi-smallSat missions. For example, an im-
 531 portant science goal that can be addressed by an interplanetary multi-CubeSat mission
 532 would be the latitudinal extent of SEP events (Dresing et al., 2012; Desai & Giacalone,
 533 2016) The AGILE team looks forward to a successful launch and analysis of data col-
 534 lected.

535 Acknowledgments

536 This work was funded by the Heliophysics Technology and Instrument Development for
 537 Science (HTIDS) ITD and LNAPP program in response to NASA Research Announce-
 538 ment (NRA) NNH18ZDA001N-HTIDS for Research Opportunities in Space and Earth
 539 Science-2018 (ROSES-2018).

540 All the authors declare no financial or other conflicts of interest. This paper de-
 541 scribes a in-situ space instrument and contains all relevant information. The AGILE team
 542 thanks Tom Flatley and the GenSat-1 team for providing a CubeSat platform, engineer-
 543 ing and data downlink support.

544 References

- 545 Agotstinelli, e. a. (2003). Geant4 simulation toolkit. *Nuclear Instruments*
 546 *and Methods in Physics Research Section A: Accelerators, Spectrometers,*
 547 *Detectors and Associated Equipment*, 506(3), 250-303. Retrieved from
 548 <http://www.sciencedirect.com/science/article/pii/S0168900203013688>
 549 doi: [https://doi.org/10.1016/S0168-9002\(03\)01368-8](https://doi.org/10.1016/S0168-9002(03)01368-8)
- 550 Ammerlaan, C., Rumphorst, R., & Koerts, L. (1963). Particle identifica-
 551 tion by pulse shape discrimination in the p-i-n type semiconductor de-
 552 tector. *Nuclear Instruments and Methods*, 22, 189-200. Retrieved from
 553 <https://www.sciencedirect.com/science/article/pii/0029554X63902489>
 554 doi: [https://doi.org/10.1016/0029-554X\(63\)90248-9](https://doi.org/10.1016/0029-554X(63)90248-9)
- 555 Baker, D. N., Erickson, P. J., Fennell, J. F., Foster, J. C., Jaynes, A. N., & Verro-
 556 nen, P. (2018). Space weather effects in the earth's radiation belts. *Space Sci*
 557 *Rev*, 214, 17. doi: 0.1007/s11214-017-0452-7
- 558 Baker, D. N., Jaynes, A. N., Kanekal, S. G., Foster, J. C., Erickson, P. J., Fennell,
 559 J. F., ... Wygant, J. R. (2016). Highly relativistic radiation belt electron
 560 acceleration, transport, and loss: Large solar storm events of march and june
 561 2015. *Journal of Geophysical Research: Space Physics*, 121(7), 6647-6660.
 562 Retrieved from [https://agupubs.onlinelibrary.wiley.com/doi/abs/](https://agupubs.onlinelibrary.wiley.com/doi/abs/10.1002/2016JA022502)
 563 [10.1002/2016JA022502](https://doi.org/10.1002/2016JA022502) doi: <https://doi.org/10.1002/2016JA022502>
- 564 Blake, J., & Friesen, L. (1977). A technique to determine the charge state of the
 565 anomalous low-energy cosmic rays. In *15th international cosmic ray conference*
 566 (Vol. 2, p. 341).
- 567 Carboni, S., Barlini, S., Bardelli, L., Le Neindre, N., Bini, M., Borderie, B., ...
 568 Fazia Collaboration (2012, February). Particle identification using the delta
 569 E-E technique and pulse shape discrimination with the silicon detectors of the
 570 FAZIA project. *Nuclear Instruments and Methods in Physics Research A*,
 571 664(1), 251-263. doi: 10.1016/j.nima.2011.10.061
- 572 Cenna, F., Cartiglia, N., Friedl, M., Kolbinger, B., Sadrozinski, H.-W., Seiden, A.,
 573 ... Zatserklyaniy, A. (2015). Weightfield2: A fast simulator for silicon and

- 574 diamond solid state detector. *Nuclear Instruments and Methods in Physics*
 575 *Research Section A: Accelerators, Spectrometers, Detectors and Associated*
 576 *Equipment*, 796, 149-153. Retrieved from [https://www.sciencedirect.com/](https://www.sciencedirect.com/science/article/pii/S0168900215004842)
 577 [science/article/pii/S0168900215004842](https://www.sciencedirect.com/science/article/pii/S0168900215004842) (Proceedings of the 10th Interna-
 578 tional Conference on Radiation Effects on Semiconductor Materials Detectors
 579 and Devices) doi: <https://doi.org/10.1016/j.nima.2015.04.015>
- 580 Council, N. R. (2004). *Plasma physics of the local cosmos*. Washington, DC: The
 581 National Academies Press. Retrieved from [https://www.nap.edu/catalog/](https://www.nap.edu/catalog/10993/plasma-physics-of-the-local-cosmos)
 582 [10993/plasma-physics-of-the-local-cosmos](https://www.nap.edu/catalog/10993/plasma-physics-of-the-local-cosmos) doi: 10.17226/10993
- 583 Cummings, J. R., Cummings, A. C., Mewaldt, R. A., Selesnick, R. S., Stone, E. C.,
 584 & von Rosenvinge, T. T. (1993). New evidence for geomagnetically trapped
 585 anomalous cosmic rays. *Geophysical Research Letters*, 20(18), 2003-2006.
 586 Retrieved from [https://agupubs.onlinelibrary.wiley.com/doi/abs/](https://agupubs.onlinelibrary.wiley.com/doi/abs/10.1029/93GL01961)
 587 [10.1029/93GL01961](https://agupubs.onlinelibrary.wiley.com/doi/abs/10.1029/93GL01961) doi: <https://doi.org/10.1029/93GL01961>
- 588 Desai, M., & Giacalone, J. (2016, December). Large gradual solar energetic particle
 589 events. *Living Reviews in Solar Physics*, 13(1). (Publisher Copyright: The
 590 Author(s) 2016. Copyright: Copyright 2021 Elsevier B.V., All rights reserved.)
 591 doi: 10.1007/s41116-016-0002-5
- 592 Dresing, N., Gómez-Herrero, R., Klassen, A., Heber, B., Kartavykh, Y., & Dröge,
 593 W. (2012). The large longitudinal spread of solar energetic particles
 594 during the 17 January 2010 solar event. *Solar Physics*, 281(1), 281-300.
 595 Retrieved from <https://doi.org/10.1007/s11207-012-0049-y> doi:
 596 [10.1007/s11207-012-0049-y](https://doi.org/10.1007/s11207-012-0049-y)
- 597 Falthammar, C.-G. (1965). Effects of time-dependent electric fields on geomagneti-
 598 cally trapped radiation. *Journal of Geophysical Research (1896-1977)*, 70(11),
 599 2503-2516. Retrieved from [https://agupubs.onlinelibrary.wiley.com/](https://agupubs.onlinelibrary.wiley.com/doi/abs/10.1029/JZ070i011p02503)
 600 [doi/abs/10.1029/JZ070i011p02503](https://agupubs.onlinelibrary.wiley.com/doi/abs/10.1029/JZ070i011p02503) doi: [https://doi.org/10.1029/](https://doi.org/10.1029/10.1029/JZ070i011p02503)
 601 [JZ070i011p02503](https://doi.org/10.1029/JZ070i011p02503)
- 602 Fennell, J. F., Roeder, J. L., Kurth, W. S., Henderson, M. G., Larsen, B. A., Hospo-
 603 darsky, G., ... Reeves, G. D. (2014). Van allen probes observations of direct
 604 wave-particle interactions. *Geophysical Research Letters*, 41(6), 1869-1875.
 605 Retrieved from [https://agupubs.onlinelibrary.wiley.com/doi/abs/](https://agupubs.onlinelibrary.wiley.com/doi/abs/10.1002/2013GL059165)
 606 [10.1002/2013GL059165](https://agupubs.onlinelibrary.wiley.com/doi/abs/10.1002/2013GL059165) doi: <https://doi.org/10.1002/2013GL059165>
- 607 Gautier, F., Greeley, A., S.G., K., T., Isidori, Legras, A., Minafra, N., ... Schiller,
 608 Q. (2021). A novel technique for real-time ion identification and energy mea-
 609 surement for in situ space instrumentation. *arXiv:2103.00613*. Retrieved from
 610 <https://arxiv.org/abs/2103.00613>
- 611 Goulding, & Harvey. (1975).
 612 *Annual Review of Nuclear Science*, 25, 167-240. Retrieved from [https://doi](https://doi.org/10.1146/annurev.ns.25.120175.001123)
 613 [.org/10.1146/annurev.ns.25.120175.001123](https://doi.org/10.1146/annurev.ns.25.120175.001123)
- 614 Haller, G., & Wooley, B. (1994). A 700-mhz switched-capacitor analog waveform
 615 sampling circuit. *IEEE Journal of Solid-State Circuits*, 29(4), 500-508. doi: 10
 616 .1109/4.280700
- 617 Horne, R., Thorne, R., Shprits, Y., Meredith, N., Glauert, S., Smith, A., ... De-
 618 creau, P. (2005, 10). Wave acceleration of electrons in the van allen radiation
 619 belts. *Nature*, 437, 227-30. doi: 10.1038/nature03939
 620 <https://www.caen.it/products/a7508/>. (n.d.). Retrieved from <https://www.caen>
 621 [.it/products/a7508/](https://www.caen.it/products/a7508/) (Rev. 1)
- 622 Jaynes, A. N., Baker, D. N., Singer, H. J., Rodriguez, J. V., Loto'aniu, T. M., Ali,
 623 A. F., ... Reeves, G. D. (2015). Source and seed populations for relativistic
 624 electrons: Their roles in radiation belt changes. *Journal of Geophysi-
 625 cal Research: Space Physics*, 120(9), 7240-7254. Retrieved from [https://](https://agupubs.onlinelibrary.wiley.com/doi/abs/10.1002/2015JA021234)
 626 agupubs.onlinelibrary.wiley.com/doi/abs/10.1002/2015JA021234 doi:
 627 <https://doi.org/10.1002/2015JA021234>

- 628 Kanekal, S. G., Baker, D. N., Henderson, M. G., Li, W., Fennell, J. F., Zheng,
629 Y., ... Kletzing, C. A. (2015). Relativistic electron response to the com-
630 bined magnetospheric impact of a coronal mass ejection overlapping with
631 a high-speed stream: Van allen probes observations. *Journal of Geophys-
632 ical Research: Space Physics*, 120(9), 7629-7641. Retrieved from [https://
633 agupubs.onlinelibrary.wiley.com/doi/abs/10.1002/2015JA021395](https://agupubs.onlinelibrary.wiley.com/doi/abs/10.1002/2015JA021395) doi:
634 <https://doi.org/10.1002/2015JA021395>
- 635 Kanekal, S. G., Blum, L., Christian, E. R., Crum, G., Desai, M., Dumonthier, J., ...
636 Summerlin, E. J. (2019). The merit onboard the ceres: A novel instrument
637 to study energetic particles in the earth's radiation belts. *Journal of Geophys-
638 ical Research: Space Physics*, 124(7), 5734-5760. Retrieved from [https://
639 agupubs.onlinelibrary.wiley.com/doi/abs/10.1029/2018JA026304](https://agupubs.onlinelibrary.wiley.com/doi/abs/10.1029/2018JA026304) doi:
640 <https://doi.org/10.1029/2018JA026304>
- 641 Klecker. (2009). Energetic particles in the heliosphere. In *21st european cosmic ray
642 symposium* (p. 27-38).
- 643 Klecker, B. (1999). Anomalous cosmic rays: Our present understanding
644 and open questions. *Advances in Space Research*, 23(3), 521-530. Re-
645 trieved from [https://www.sciencedirect.com/science/article/pii/
646 S0273117799800064](https://www.sciencedirect.com/science/article/pii/S0273117799800064) (The Transport of Galactic and Anomalous Cos-
647 mic Rays in the Heliosphere: Observations, Simulations and Theory) doi:
648 [https://doi.org/10.1016/S0273-1177\(99\)80006-4](https://doi.org/10.1016/S0273-1177(99)80006-4)
- 649 Kleinfelder, S. (1988). Development of a switched capacitor based multi-channel
650 transient waveform recording integrated circuit. *IEEE Transactions on Nuclear
651 Science*, 35(1), 151-154. doi: 10.1109/23.12695
- 652 Leske, R., Cummings, A., R.A., M., & Stone, E. C. (2013). Anomalous and galac-
653 tic cosmic rays at 1 au during the cycle 23/24 solar minimum. *Space Sci Rev*,
654 176, 253-263. doi: <https://doi.org/10.1007/s11214-011-9772-1>
- 655 Leske, R. A., Mewaldt, R. A., Stone, E. C., & von Rosenvinge, T. T. (2001). Obser-
656 vations of geomagnetic cutoff variations during solar energetic particle events
657 and implications for the radiation environment at the space station. *Journal
658 of Geophysical Research: Space Physics*, 106(A12), 30011-30022. Retrieved
659 from [https://agupubs.onlinelibrary.wiley.com/doi/abs/10.1029/
660 2000JA000212](https://agupubs.onlinelibrary.wiley.com/doi/abs/10.1029/2000JA000212) doi: <https://doi.org/10.1029/2000JA000212>
- 661 Li, X., Selesnick, R. S., Baker, D. N., Jaynes, A. N., Kanekal, S. G., Schiller, Q.,
662 ... Blake, J. B. (2015). Upper limit on the inner radiation belt mev electron
663 intensity. *Journal of Geophysical Research: Space Physics*, 120(2), 1215-1228.
664 Retrieved from [https://agupubs.onlinelibrary.wiley.com/doi/abs/
665 10.1002/2014JA020777](https://agupubs.onlinelibrary.wiley.com/doi/abs/10.1002/2014JA020777) doi: <https://doi.org/10.1002/2014JA020777>
- 666 Mann, I., Ozeke, L., Murphy, K., Claudepierre, S. G., Turner, D. L., Baker,
667 D. N., ... Honary, F. (2016). Explaining the dynamics of the ultra-
668 relativistic third van allen radiation belt. *Nature Phys*, 12, 978-983. doi:
669 <https://doi.org/10.1038/nphys3799>
- 670 Mutterer, M., Trzaska, W. H., Tyurin, G. P., Evsenin, A. V., von Kalben, J., Kem-
671 mer, J., ... Khlebnikov, S. V. (2000). Breakthrough in pulse-shape based
672 particle identification with silicon detectors. *IEEE Transactions on Nuclear
673 Science*, 47(3), 756-759. doi: 10.1109/23.856510
- 674 Oberla, E., Genat, J.-F., Grabas, H., Frisch, H., Nishimura, K., & Varner, G. (2014).
675 A 15gsa/s, 1.5ghz bandwidth waveform digitizing ASIC. *Nuclear Instruments
676 and Methods in Physics Research Section A: Accelerators, Spectrometers, De-
677 tectors and Associated Equipment*, 735, 452-461. Retrieved from [https://
678 www.sciencedirect.com/science/article/pii/S016890021301276X](https://www.sciencedirect.com/science/article/pii/S016890021301276X) doi:
679 <https://doi.org/10.1016/j.nima.2013.09.042>
- 680 Reames, D. (1999). Particle acceleration at the sun and in the heliosphere. *Space
681 Science Reviews*, 90, 413-491.

- 682 Reames, D. (2017). *Solar energetic particles* (Vol. 932). doi: 10.1007/978-3-319
683 -50871-9
- 684 Reames, D. (2020). Distinguishing the rigidity dependences of acceleration and
685 transport in solar energetic particles. *Sol Phys*, 295, 113. doi: [https://doi.org/
686 10.1007/s11207-020-01680-6](https://doi.org/10.1007/s11207-020-01680-6)
- 687 Reeves, G. D., Spence, H. E., Henderson, M. G., Morley, S. K., Friedel, R. H. W.,
688 Funsten, H. O., ... Niehof, J. T. (2013). Electron acceleration in the heart
689 of the van allen radiation belts. *Science*, 341(6149), 991–994. Retrieved
690 from <https://science.sciencemag.org/content/341/6149/991> doi:
691 10.1126/science.1237743
- 692 Scholer, M. (1975). Transport of energetic solar particles on closed magnetospheric
693 field lines. *Space Science Reviews*, 17, 3-44.
- 694 Schulz, M., & Lanzerotti, L. J. (1974). *Particle Diffusion in the Radiation Belts*.
695 New York: Springer.
- 696 Selesnick, R. S., Cummings, A. C., Cummings, J. R., Mewaldt, R. A., Stone, E. C.,
697 & von Rosenvinge, T. T. (1995). Geomagnetically trapped anomalous cosmic
698 rays. *Journal of Geophysical Research: Space Physics*, 100(A6), 9503-9518.
699 Retrieved from [https://agupubs.onlinelibrary.wiley.com/doi/abs/
700 10.1029/94JA03140](https://agupubs.onlinelibrary.wiley.com/doi/abs/10.1029/94JA03140) doi: <https://doi.org/10.1029/94JA03140>
- 701 Shprits, Y. Y., Elkington, S. R., Meredith, N. P., & Subbotin, D. A. (2008). Review
702 of modeling of losses and sources of relativistic electrons in the outer radiation
703 belt i: Radial transport. *Journal of Atmospheric and Solar-Terrestrial Physics*,
704 70(14), 1679-1693. Retrieved from [https://www.sciencedirect.com/
705 science/article/pii/S1364682608001648](https://www.sciencedirect.com/science/article/pii/S1364682608001648) (Dynamic Variability of Earth's
706 Radiation Belts) doi: <https://doi.org/10.1016/j.jastp.2008.06.008>
- 707 Stilwell, D. E., Davis, W. D., Joyce, R. M., McDonald, F. B., Trainor, J. H.,
708 Althouse, W. E., ... Vogt, R. E. (1979). The voyager cosmic ray ex-
709 periment. *IEEE Transactions on Nuclear Science*, 26(1), 513-520. doi:
710 10.1109/TNS.1979.4329683
- 711 Stoffregen, P. J., & Coon, R. (2014). Teensy usb development board. *Code Library*.
712 Retrieved from <https://www.pjrc.com/teensy/>
- 713 Stone, E. C., Cohen, C. M. S., Cook, W. R., Cummings, A. C., Gauld, B., Kecman,
714 B., ... Olevitch, M. A. (1998a). The cosmic ray isotope spectrometer for the
715 advanced composition explorer. *Space Sci. Rev.*, 86, 285.
- 716 Stone, E. C., Cohen, C. M. S., Cook, W. R., Cummings, A. C., Gauld, B., Kec-
717 man, B., ... von Rosenvinge, T. T. (1998b). The solar isotope spectrometer
718 for the advanced composition explorer. *Space Science Reviews*, 86(1), 357–
719 408. Retrieved from <https://doi.org/10.1023/A:1005027929871> doi:
720 10.1023/A:1005027929871
- 721 Stone, E. C., Vogt, R. E., McDonald, F. B., Teegarden, B. J., Trainor, J. H.,
722 Jokipii, J. R., & Webber, W. R. (1977). Cosmic ray investigation for
723 the voyager missions; energetic particle studies in the outer heliosphere—
724 and beyond. *Space Science Reviews*, 21(3), 355–376. Retrieved from
725 <https://doi.org/10.1007/BF00211546> doi: 10.1007/BF00211546
- 726 Thorne, R. M. (2010). Radiation belt dynamics: The importance of wave-particle
727 interactions. *Geophysical Research Letters*, 37(22). Retrieved from [https://
728 agupubs.onlinelibrary.wiley.com/doi/abs/10.1029/2010GL044990](https://agupubs.onlinelibrary.wiley.com/doi/abs/10.1029/2010GL044990) doi:
729 <https://doi.org/10.1029/2010GL044990>
- 730 Turner, D. L., O'Brien, T. P., Fennell, J. F., Claudepierre, S. G., Blake, J. B.,
731 Jaynes, A. N., ... Reeves, G. D. (2017). Investigating the source of near-
732 relativistic and relativistic electrons in earth's inner radiation belt. *Jour-
733 nal of Geophysical Research: Space Physics*, 122(1), 695-710. Retrieved
734 from [https://agupubs.onlinelibrary.wiley.com/doi/abs/10.1002/
735 2016JA023600](https://agupubs.onlinelibrary.wiley.com/doi/abs/10.1002/2016JA023600) doi: <https://doi.org/10.1002/2016JA023600>

- 736 von Roseninge, T. T., Reames, D. V., Baker, R., Hawk, J., Nolan, J. T., Ryan, L.,
737 ... Wiedenbeck, M. E. (2008). The high energy telescope for stereo. *Space Sci-*
738 *ence Reviews*, 136(1), 391–435. Retrieved from [https://doi.org/10.1007/](https://doi.org/10.1007/s11214-007-9300-5)
739 [s11214-007-9300-5](https://doi.org/10.1007/s11214-007-9300-5) doi: 10.1007/s11214-007-9300-5
- 740 Zhao, H., Baker, D. N., Li, X., Jaynes, A. N., & Kanekal, S. G. (2018). The ac-
741 celeration of ultrarelativistic electrons during a small to moderate storm of
742 21 april 2017. *Geophysical Research Letters*, 45(12), 5818–5825. Retrieved
743 from [https://agupubs.onlinelibrary.wiley.com/doi/abs/10.1029/](https://agupubs.onlinelibrary.wiley.com/doi/abs/10.1029/2018GL078582)
744 [2018GL078582](https://doi.org/10.1029/2018GL078582) doi: <https://doi.org/10.1029/2018GL078582>